



Theoretical study of hydration in $Y_2Mo_3O_{12}$: Effects on structure and negative thermal expansion

Cite as: AIP Advances 5, 027126 (2015); <https://doi.org/10.1063/1.4913361>

Submitted: 24 September 2014 . Accepted: 10 February 2015 . Published Online: 18 February 2015

Ming-Yi Wu , Lei Wang, Yu Jia, Zheng-Xiao Guo, and Qiang Sun 



View Online



Export Citation



CrossMark

ARTICLES YOU MAY BE INTERESTED IN

[First-principles study of negative thermal expansion in zinc oxide](#)

Journal of Applied Physics **114**, 063508 (2013); <https://doi.org/10.1063/1.4817902>

[Negative thermal expansion properties in tetragonal NbPO₅ from the first principles studies](#)

AIP Advances **7**, 035202 (2017); <https://doi.org/10.1063/1.4977874>

[Suppression of temperature hysteresis in negative thermal expansion compound BiNi_{1-x}Fe_xO₃ and zero-thermal expansion composite](#)

Applied Physics Letters **106**, 061912 (2015); <https://doi.org/10.1063/1.4908258>

Don't let your writing
keep you from getting
published!

AIP | Author Services

Learn more today!

Theoretical study of hydration in $Y_2Mo_3O_{12}$: Effects on structure and negative thermal expansion

Ming-Yi Wu,¹ Lei Wang,¹ Yu Jia,¹ Zheng-Xiao Guo,² and Qiang Sun^{1,a}

¹International Laboratory for Quantum Functional Materials of Henan, and School of Physics and Engineering, Zhengzhou University, Zhengzhou, 450001, China

²Department of Chemistry, University College London, London WC1H 0AJ, UK

(Received 24 September 2014; accepted 10 February 2015; published online 18 February 2015)

We report *ab-initio* calculations of water absorption in $Y_2Mo_3O_{12}$. The absorption geometry of H_2O in $Y_2Mo_3O_{12}$ and the binding property between H_2O and $Y_2Mo_3O_{12}$ have been first identified. Our calculated results show that water is chemisorbed in $Y_2Mo_3O_{12}$ with O of the water binding to the Y^{3+} cation, which is further strengthened by hydrogen bonding between each of the hydrogen atoms of H_2O and the bridge O in $Y_2Mo_3O_{12}$, shared by polyhedrons YO_6 and MoO_4 . The absorption of water leads to a reduced angle of Y-O-Mo and shortened Y-Mo distance, and consequently volume contraction of the material, almost linearly with the increasing number of water molecules per unit cell, up to eight in total. In addition, our phonon calculation show that the transverse vibration of Y-O-Mo is restricted due to water absorption, which in turn hinders the NTE, as it is mainly originated from this vibrational mode. Our results clarify further the fundamental mechanisms of the large volume shrinkage and the lost NTE of the framework oxide due to water absorption. © 2015 Author(s). All article content, except where otherwise noted, is licensed under a Creative Commons Attribution 3.0 Unported License. [<http://dx.doi.org/10.1063/1.4913361>]

I. INTRODUCTION

The $A_2M_3O_{12}$ family of negative thermal expansion (NTE) materials has attracted much interest in recent years (A= a trivalent transition metal or a lanthanide from Lu to Ho, M= W^{6+} or Mo^{6+}). These materials are characterized by great chemical flexibility and a phase transition from the low-temperature monoclinic to the high-temperature orthorhombic structure.¹ Both phase structures are microporous, forming open, interstitial cation-free frameworks consisting of vertex-linked AO_6 octahedra and MO_4 tetrahedra, where each AO_6 octahedron joins MO_4 tetrahedra with sharing O of their corners. In its high-temperature orthorhombic structure, $A_2M_3O_{12}$ exhibits a negative thermal expansion (NTE) phenomenon. The reason why NTE occurs is still under debate. The study of other NET materials, e.g. ZrW_2O_8 , suggested that NTE is due to the transverse thermal vibrations perpendicular to the Zr-O-W linkage that cause contraction in these materials.²⁻⁶ However, recently, Bridges *et al.*⁷ argued that the Zr-O-W linkage is relatively stiff and does not permit bending. They propose that the low energy vibrational modes that lead to negative thermal expansion involve correlated rotations of ZrO_6 octahedra and WO_4 tetrahedra that produce large $\langle 111 \rangle$ translations of the WO_4 tetrahedra. Different from ZrW_2O_8 , polyhedra of $A_2M_3O_{12}$ undergoes some slight distortions besides vibrations, i.e. semi-rigid.^{8,9} Another proposed suggestion for $A_2M_3O_{12}$ is that a change of balance in atomic-level mechanisms contributes to expansion and reduction of inter-atomic distances.¹⁰ They found that the reductions of the Y-Mo non-bonding distance and the Y-O-Mo angles are the basic structural features that provoke NTE in $Y_2Mo_3O_{12}$ and other isostructural compounds. Theoretical result¹¹ indicates that it is the substantial effect of the vibrations of the bridge O atom in the Y-O-Mo linkage which plays a crucial role in the NTE. Meanwhile, these

^aCorrespondence to: qsun@zzu.edu.cn

vibrations also lead to the distortion of the YO_6 octahedron and MoO_4 tetrahedron, and hence, contraction in volume.

Experiment shows that the size of the A^{3+} cation in $A_2M_3O_{12}$ affects the performance of the NTE. Axial thermal expansion coefficient calculated from high temperature X-ray diffraction (RT-1073K) showed that as the size of A^{3+} cation decreases, the volume thermal expansion coefficient and the linear thermal expansion coefficient become less negative.¹² Therefore, Y^{3+} , which have the largest ionic radius of all trivalent transition elements, makes $Y_2Mo_3O_{12}$ as the most promising NTE candidate in the $A_2M_3O_{12}$ family. In particular, experiment confirms that $Y_2Mo_3O_{12}$ exhibits NTE in a large temperature range (473 ~ 1173 K) and the overall linear coefficient of thermal expansion ($\alpha_l = \alpha_v/3$) is -1.26×10^{-5} .¹

Though the NTE property of the oxide materials have important potential applications and many studies have focused on the mechanisms for the NTE, this phenomenon (NTE) ceases to exist after many tungstates and molybdates of the $A_2M_3O_{12}$ family keenly absorb water and transforming to a stable trihydrate structure, accompanied by a volume shrinkage, therefore, hindering its practical applications.^{1,12,14-21} In another framework structure oxides of ZrW_2O_8 , N. Duan, *et al.* first reported the hydration phenomenon, and showed that water absorption causes a dramatic decrease in the unit cell size of ZrW_2O_8 .¹³ Sumithra *et al.* briefly reported that the cell volume of the hydrated $Y_2W_3O_{12}$ is 7% smaller than the un-hydrated, and speculated that the hydration suppresses the transverse vibrations at room temperature and the removal of the water also confirm that some vibrational modes, which lead to the NTE, were missing in the hydrated structure.²⁰ Because of the presence of water, degeneracy of the Raman bands exists for symmetric stretching, asymmetric stretching, and the bending modes. However, the lattice translational modes cannot be observed.²¹ In the meantime, Liang *et al.*²¹ demonstrate that the presence of water species hinders not only the rocking motion but also other types of motion of the corner-shared polyhedra. However, few investigations have been reported on the absorption geometry and the binding properties between H_2O and $Y_2Mo_3O_{12}$, and the reasons of the volume shrinkage and the disappearing of the NTE in $Y_2Mo_3O_{12}$ due to hydration in atomic level. All these problems are difficult to be solved by experiments. Therefore, further studies are still necessary to clarify these puzzles and underlying mechanism in details. In this paper, we attempt to study H_2O absorption in $Y_2Mo_3O_{12}$ by first-principles calculations, in order to provide further theoretical insight of the effects of water absorption on the structure, volume, phonon properties as well as NTE of the material.

II. METHODOLOGY

To investigate H_2O molecule absorption in $Y_2Mo_3O_{12}$, first-principles calculations were performed using the Vienna *ab-initio* simulation package (VASP)^{22,23} within the framework of density functional theory (DFT).^{24,25} The projector augmented wave (PAW) method was used to describe the interaction between valence and core electrons.^{26,27} For the treat of the electron exchange and correlation interaction, three different approximation functionals were tested: LDA, GGA_PBE and vdW-DF2,²⁷ and the results are listed in Table I. Compared with the lattice parameters from experiment data and considered the existence of hydrogen bonds, vdW-DF2 functional gave a more reliable result, therefore, further calculations were carried out based on this functional. The Kohn-Sham orbitals are expanded in a plane wave basis set with a cutoff energy of 550 eV. Monkhorst-Pack

TABLE I. Structural parameters of $Y_2Mo_3O_{12}$ unit cell calculated using different functionals. Experimental values are given for comparison. Values in brackets are the difference between calculated and experimental values in percentage.

	a (Å)	b (Å)	c (Å)
Experiment	13.869 ^a	9.935 ^a	10.022 ^a
LDA	14.02(1.09%)	10.05(1.16%)	10.19(1.68%)
GGA_PBE	14.15(2.03%)	10.16(2.26%)	10.37(3.47%)
vdW	13.93(0.44%)	10.05(1.16%)	10.18(1.58%)

^aExperimental data from Reference 1.

scheme with $2 \times 2 \times 2$ k-point sampling in the Brillouin zone were used for the structure relaxation.²⁸ This set has been tested to be sufficient for our calculation. The volume of the unit cell was not fixed during structure relaxation because both the volume and the structure of $Y_2Mo_3O_{12}$ change during hydration. The Fermi level was smeared by the Methfessel and Paxton approach with a Gaussian smearing width of 0.02 eV.²⁹ Energy differences were converged within 10^{-8} eV, and the forces on the relaxed atoms were less than 10^{-4} eV/Å. The phonon spectra were calculated using PHONOPY1.6.2 software developed by Parlinski.³⁰ In the phonon calculations, a $1 \times 1 \times 2$ super-cell was used within the frozen-phonon method. The applied displacement was 0.01 Å. For the calculation of the phonon density of states, integrations over the Brillouin zone of the cuboid crystal were sampled with a $2 \times 2 \times 2$ mesh of k-points generated by Monkhorst-Pack scheme.

III. RESULTS AND DISCUSSION

A. Geometric structures and energies

The initial step of our research is to determine the structural characteristics of $Y_2Mo_3O_{12}$. The orthorhombic structure is fully relaxed using three different functionals as listed in Table I. Compared with the experimental data, PBE functional overestimates more than 2.03%, which is twice as large as LDA and vdW-DF2. This is an accepted error in PBE for it softens the bond, leading to increased lattice parameters.³¹ Furthermore, it often fails on modeling highly coordinated atoms, such as Mo, because it also includes a scaled gradient in its enhancement factor.³² Among all, the vdW-DF2 functional is the best approach because it combines the revPBE for exchange energy, and LDA and nonlocal electron correlation for correlation energy.³³ The error of calculated lattice parameter along an axis is even limited to 0.44%. All the results give us the confidence of using vdW-DF2 functional to interpret the properties of water absorption in $Y_2Mo_3O_{12}$.

To investigate the water absorption behavior in $Y_2Mo_3O_{12}$, one water molecule is absorbed on two different hollow sites in the first step: near Y and Mo atoms, denoted as site 1 (Fig. 1(a)) and site 2 (Fig. 1(b)), respectively. The stability is determined by the absorption energy defined as follows:

$$E_{absorption} = E_{H_2O+Y_2Mo_3O_{12}} - E_{H_2O} - E_{Y_2Mo_3O_{12}}, \quad (1)$$

The energy of an H_2O molecule has been calculated as in gas phase: We put it in a $10\text{Å} \times 10\text{Å} \times 10\text{Å}$ cubic box, and then calculate the energy of H_2O molecule. The absorption energies in both sites are less than -0.40 eV, suggesting water could strongly bond to the $Y_2Mo_3O_{12}$ compound and form a stable hydride structure. Site 1 is more stable than site 2 by -0.15 eV. The reason why water is more keen to absorb on the site 1 can be explained by Lei Wang *et al.*¹¹ They reported that the Y-O bond is more ionic character, while Mo-O is more covalent due to a remarkable charge overlapping between Mo and O atoms, hence, Y is more attractive to water than Mo.

The water absorption also shifts the relevant position of the YO_6 octahedra joining MoO_4 tetrahedra, as shown in Fig. 2. The figure provides the bond lengths and angles of the water with the relevant YO_6 and Mo_4 polyhedra. The Y-Y distance is contracted from 6.23 to 5.92 Å. Meanwhile, all the joints are also moved towards the water in the directions of the arrows, along with the angle changes. Hence the volume of the unit cell is shrunk to 98.78% after absorption of just one H_2O molecule.

For further investigation of water absorption, up to 6 water molecules were considered here. The average absorption energy $E_{average}$ per H_2O molecule is calculated by

$$E_{average} = (E_{nH_2O+Y_2Mo_3O_{12}} - nE_{H_2O} - E_{Y_2Mo_3O_{12}}) / n, \quad (2)$$

and the results are showed in Fig. 3(a) with the unit cell volume changes in percentage. Table II presents the calculated lattice parameters with different numbers of water absorption. As the water molecules increase, the average absorption energy decreases until five H_2O molecules are absorbed in the system, i.e. the $Y_2Mo_3O_{12}$ has the tendency of absorbing more water in the moisturized environment. At the same time, the unit cell contracts almost linearly with the number of absorbed water molecules, with a contraction rate by 0.75% per water molecule (see Fig. 3(a)). When 6 water molecules are added, the volume is reduced by 4.94%. Therefore, it might be expected that the

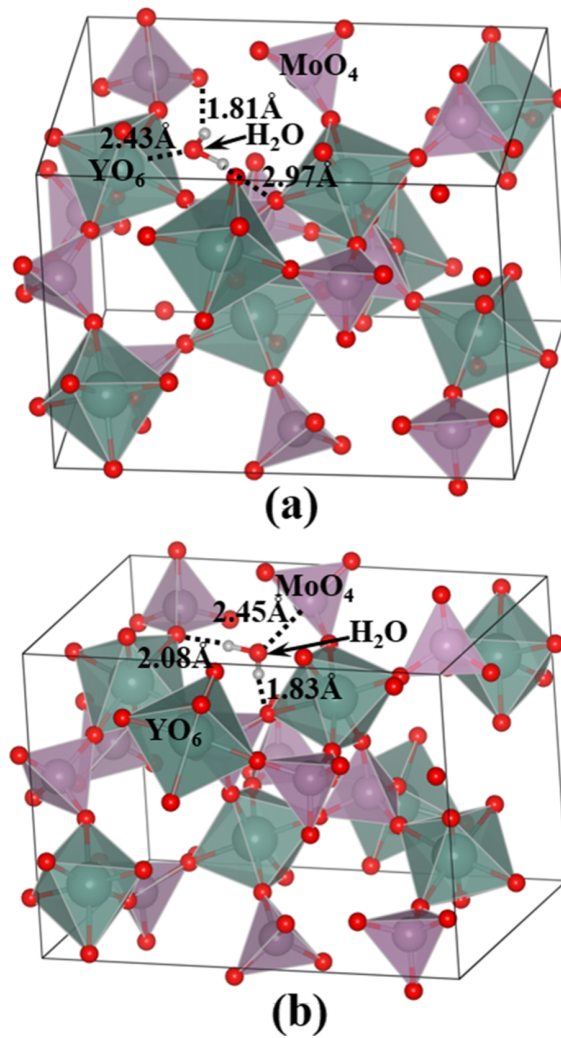


FIG. 1. One H_2O molecule absorbed in $\text{Y}_2\text{Mo}_3\text{O}_{12}$ at: (a) site 1 with absorption energy -0.55 eV; and (b) site 2 with absorption energy -0.40 eV, respectively.

volume could shrink by 6.59 % when all the eight Y atoms in the unit cell were hydrated. However, the average absorption energy does not follow this linear trend afterwards, but goes up when $\text{Y}_2\text{Mo}_3\text{O}_{12}$ absorbs six water molecules. Lattice parameters of different structures with different number of absorbed water molecules in a unit cell are given in Fig. 3(b). It can be seen that a and b

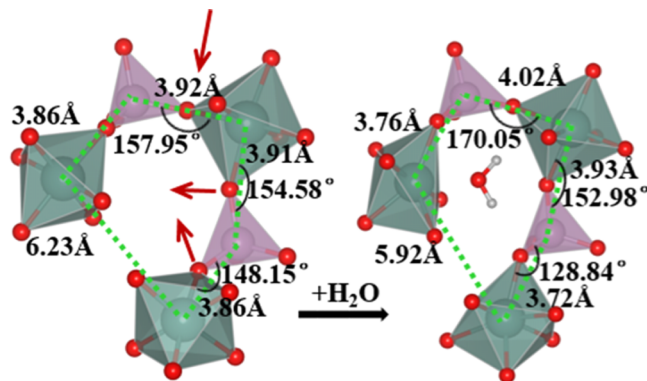


FIG. 2. Local structure of $\text{Y}_2\text{Mo}_3\text{O}_{12}$ before and after H_2O absorption.

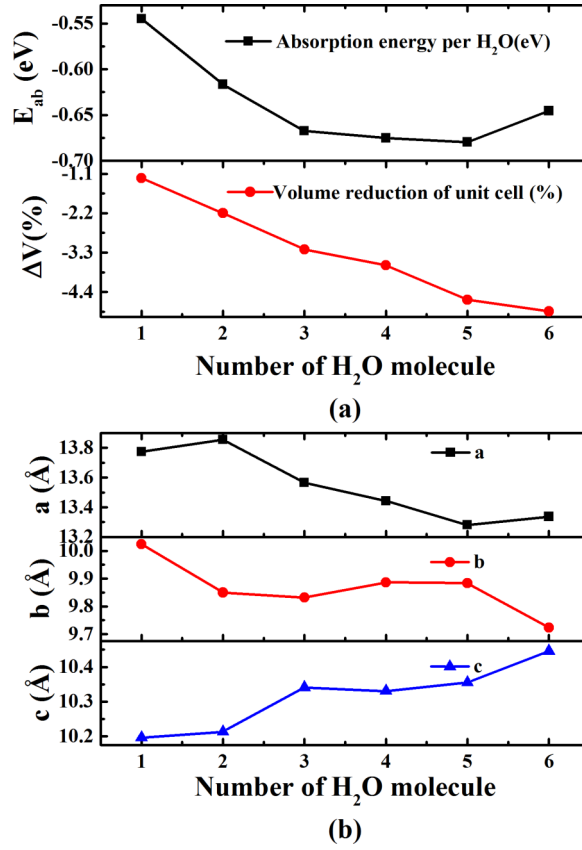


FIG. 3. Calculated (a) average absorption energy per H₂O molecule, volume shrinkage of the unit cell; and (b) the changes of lattice parameters a, b and c as the number of absorption H₂O molecules increasing from 1 to 6.

are generally decreased, while c is always increased as the number of absorption H₂O molecules increased. Meanwhile, experiment showed that the volume was contracted by 7% after absorbing water,²⁰ indicating that absorption of ~ eight water molecules per unit cell is likely the maximum.

B. Electronic properties

More direct physical insight of the binding properties between the absorbed H₂O molecule and the Y₂Mo₃O₁₂ can be obtained by the electron density difference, defined as

$$\Delta\rho = \rho(n\text{H}_2\text{O} + \text{Y}_2\text{Mo}_3\text{O}_{12}) - \rho(n\text{H}_2\text{O}) - \rho(\text{Y}_2\text{Mo}_3\text{O}_{12}), \quad (3)$$

where ρ is the space electron density. Charge decreases near the end of hybridized hydrogen atoms and accumulated near the end of the O in water molecule (O@H₂O) (see Fig. 4), resulting in an enhanced dipole in water molecule and a larger binding energy with the oxide framework material.

TABLE II. Calculated lattice parameters with different numbers of absorbed water molecules.

	a (Å)	b (Å)	c (Å)	α	β	γ	V (Å ³)
Pristine Y ₂ Mo ₃ O ₁₂	13.93	10.05	10.18	90.00°	90.00°	90.00°	1424.89
1H ₂ O@Y ₂ Mo ₃ O ₁₂	13.77	10.02	10.19	89.49°	88.94°	89.31°	1407.51
3H ₂ O@Y ₂ Mo ₃ O ₁₂	13.56	9.83	10.34	89.46°	89.26°	89.96°	1379.11
6H ₂ O@Y ₂ Mo ₃ O ₁₂	13.33	9.72	10.44	89.83°	89.51°	88.83°	1354.43

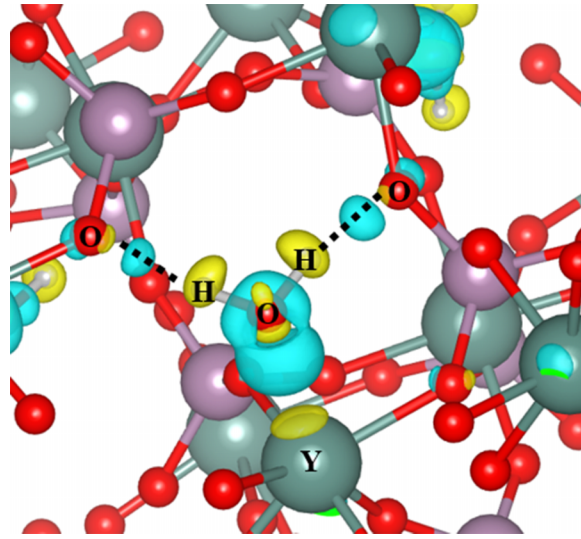


FIG. 4. 3D iso-surface plot for charge density difference of the H₂O molecule absorbed in Y₂Mo₃O₁₂. Yellow and blue surface represented charge depletion and accumulation in space, respectively. The iso-surface level is 0.005 e/Å³.

At the same time, two typical hydrogen bonds, characterized by the long distance electron dispersion, are formed along the H atom in water molecule (H@H₂O) and bridge O atoms, which shared by polyhedra YO₆ and MoO₄. Thus, H₂O molecule absorption in Y₂Mo₃O₁₂ could be accounted for by the chemical absorption between Y³⁺ cation and the O@H₂O and the O-H...O hydrogen bonds between the H@H₂O and the bridge O atom.

C. Phonon properties

To investigate how H₂O absorption hinders the vibration modes of NTE, we calculated the phonon density of states (DOS) of the systems. The phonon DOS is based on the following equation:

$$N_i(E) = \int \frac{d\vec{k}}{4\pi^2} |e_j(i)|^2 \delta[E - E_j(\vec{k})], \quad (4)$$

where e_j is the eigenvector associated with the mode of energy E_j .

The total DOSs of Y₂Mo₃O₁₂ without hydration and with 1, 3 and 6 H₂O molecules absorption are depicted in Fig. 5. The calculated dispersion of the total phonon DOS is in line with the peak positions of the Raman spectrum.²¹ We found that the phonon peak at 100 cm⁻¹ decreased after the water absorption, ranging from the 70 cm⁻¹ to 130 cm⁻¹. It has been reported that these modes show the strongest negative Grüneisen parameter and contribute most to the NTE behavior.¹¹ These modes are softening as the number of absorbed H₂O molecules increases, indicating that the vibrations that contribute to the NTE become softer. In addition, the phonon modes near 210 cm⁻¹ which have positive Grüneisen parameters rise. This result indicates that phonon modes which contribute to positive thermal expansion increase, and the thermal expansion tendency will become stronger. The phonon modes near 300 cm⁻¹, which have the negative Grüneisen parameters, also decrease as the number of H₂O absorption increases. In the range of 400-650 cm⁻¹, the phonon DOS of pristine Y₂Mo₃O₁₂ is zero, and these modes increase when H₂O is absorbed initially, and should be induced purely by the vibration of the H₂O molecules. Besides, high frequency phonon DOS peaks near 830 cm⁻¹ and 970 cm⁻¹ also decrease because of H₂O absorption. Liang *et al.* have reported that the distinct change in the symmetric and asymmetric modes at 968 and 823 cm⁻¹, and the bending mode at 323 cm⁻¹ and the negative slope of these modes with temperature after the release of water species suggest that the translational and librational motions are closely coupled with stretching and bending vibrations.²¹ Together those give rise to the negative thermal expansion. In our results, we

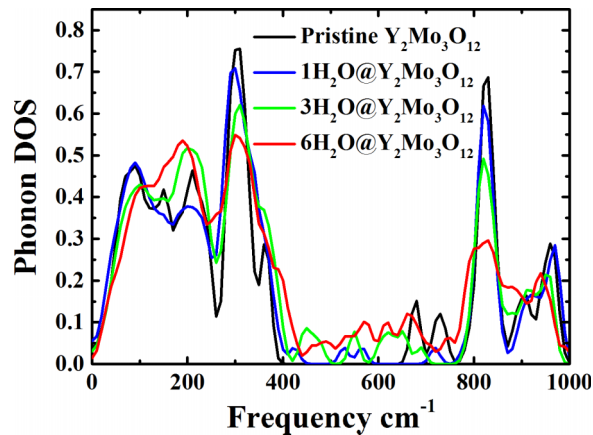


FIG. 5. The phonon density of states (DOS) of $Y_2Mo_3O_{12}$ without and with absorption of 1, 3, 6 H_2O molecules.

also found that the peaks of these modes are reduced when the number of absorbed H_2O molecules increases from 1 to 6. This suggests that the translational and librational motions which give rise to the negative thermal expansion are hindered by the absorbed H_2O molecules.

To investigate the specific variation of vibration mode after the H_2O absorption in $Y_2Mo_3O_{12}$, we also calculated the partial DOS of phonon for pristine $Y_2Mo_3O_{12}$ and $Y_2Mo_3O_{12}$ with the absorption of 1, 3 and 6 H_2O molecules, as shown in Fig. 6. The reduction of the phonon peak in 100 cm^{-1} is mainly due to the O and Mo. The DOS of Y shows little change in this range. From the calculated eigenvectors of this mode at Gamma point, we knew that this mode involves the transverse swing of the YO_6 octahedron and the MoO_4 tetrahedron, and this swing is centered on the O atom at the bridge site. When H_2O is absorbed in it, the DOS of this transverse swing is reduced because the O atom at the bridge site forms a hydrogen bond with the $H@H_2O$, which hinders the vibration of the O atom at bridge site. The increase of DOS peak around 200 cm^{-1} is mainly due to the PDOSs of Y, O and Mo. According to our calculated eigenvectors of the mode at 200 cm^{-1} , this mode involves the essential librations of the MoO_4 tetrahedron and the translations of the Y^{3+} ions. When H_2O is absorbed, the transverse vibration of H_2O molecules put in motion of the bridge site O atom, which is drawn towards the H_2O . As results, the transverse vibration of H_2O promotes the librations of the MoO_4 tetrahedron, and the translations of Y^{3+} ions. The decrease of phonon peak at 295 cm^{-1} is mainly due to the decrease of PDOSs of Mo and O. We found that this mode involved

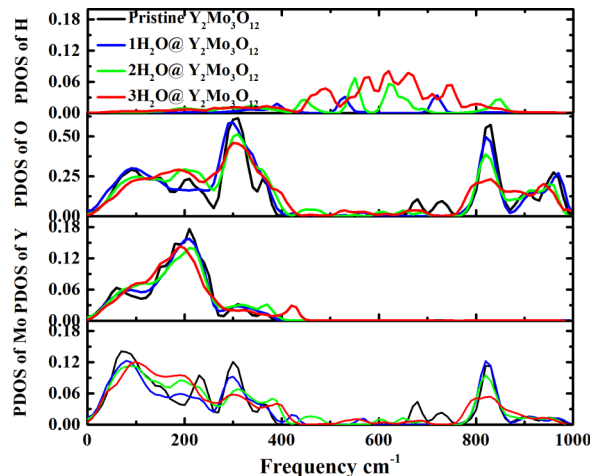


FIG. 6. Partial phonon density of states (PDOS) of $Y_2Mo_3O_{12}$ without and with absorption of 1, 3, 6 H_2O molecules.

the bending modes of the MoO₄ tetrahedral units is weakly coupled with the translations of Y³⁺ ions in Y₂Mo₃O₁₂. When H₂O absorbed in Y₂Mo₃O₁₂, the direction of the transverse vibration of the H₂O molecules is not same as that of the vibration of the O atom at the bridge site of the MoO₄ tetrahedron, so this mode hinders the bending modes of the MoO₄ tetrahedral units. The appearance of phonon peak between 400 cm⁻¹ and 650 cm⁻¹ is mainly due to the PDOS of H atom: however, the PDOSs of Y, Mo, and O are not increased evidently. The phonon mode at 600 cm⁻¹ is the swing modes of the H@H₂O from the results of calculated eigenvector of those modes. The DOSs of these modes will be increased as the number of absorbed H₂O increases. The decrease of the phonon DOS peak at 840 cm⁻¹ is mainly due to the decrease of the PDOS peak of the O atom and the Mo atom. The calculated eigenvector of this mode show that this mode corresponds the asymmetric stretching mode of the MoO₄ tetrahedron, which is consistent with the Raman analysis.²¹ We found that the stretching direction of the H@H₂O is opposite to that of the stretching of a neighboring O atom in the MoO₄ tetrahedron. Both of these two stretching motions would be weakened because of the hydrogen bonding between H@H₂O and the O@MoO₄. The decrease of phonon DOS peak at 960 cm⁻¹ is due to the reduction of the PDOS peak of the O atom. In pristine Y₂Mo₃O₁₂, this mode is essentially the symmetric stretching mode of the O@MoO₄ from the eigenvector calculated results. We found that this mode disappears when the H₂O is absorbed, which can be interpreted by the fact that the presence of the hydrogen bonding between the H@H₂O and O@MoO₄ hinders the symmetric stretching mode O@MoO₄. These findings are consistent with the existing experimental results²¹ and should assist further exploration and development of NET materials.

Finally, we would like to point out that though the hydration of the Y₂Mo₃O₁₂ is undesirable for NTE-based considerations, the specific “hydration induced volume contraction” as a function of water content may also be regarded as a “Negative Hydration Expansion (NHE)”, as opposed to the usual expansion due to hydration. Even more interestingly, such NHE is tunable by water content. This tunable NHE phenomenon might be useful to design a small negative tolerance for precision fitting and a very tight fitting could be achieved through dehydration. It might also be used as a mechanism for molecular sensing.

IV. CONCLUSIONS

By means of first-principles simulations, we have probed further the absorption of water in Y₂Mo₃O₁₂, and the effectiveness of water molecules in “damping” the vibration modes that lead to NTE. Our DFT calculations indicate that Y is the host for the water absorption, and the material could absorb up to ~ 8 water molecules per unit cell. Furthermore, the absorption of water leads to a reduced angle of Y-O-Mo, a reduced Y-Mo distance and consequently a reduced volume of the material. By calculating the phonon DOS and PDOS of Y₂Mo₃O₁₂ without and with hydration, we found that the phonon peak at 100 cm⁻¹ softens, spreading from the 70 cm⁻¹ to 130 cm⁻¹. It has been reported that these modes possess the strongest negative Grüneisen parameters and contribute most to the NTE behavior. Those modes are further softened as the number of H₂O absorption increases, indicating that the vibrations that contribute to the NTE behavior are further constrained. Combined with the calculated eigenvectors of the phonon mode at Gamma point, we found that the transverse swing mode of the YO₆ octahedron and the MoO₄ tetrahedron at 100 cm⁻¹ are softened after H₂O absorption, due to the hydrogen bonding between the O atom at the bridge site and the H@H₂O. The hydrogen bond hinders the transverse vibration of the O atom at the bridge site. In addition, the bending modes of MoO₄ tetrahedron coupled weakly with the translations of Y³⁺ ions at 295 cm⁻¹, are also softened after water absorption. As a result, the NTE, originated from these vibrational modes, is hindered. Besides these, we found that the presence of water absorption hinders the asymmetry and symmetry stretching modes of MoO₄ tetrahedra, which is consistent with the Raman analysis. Furthermore, the tunable NHE phenomenon might be useful to design a small negative tolerance for precision fitting and might also be used as a mechanism for molecular sensing.

ACKNOWLEDGMENTS

We thank Dr. Han and Dr. Shevlin at University College London for helpful discussion. MYW would like to thank Dr. Shuai Zhang, Mr. Zhenhong Wang and Mr. Zhanyu Wang for help in the numerical calculations.

- ¹ B. A. Marinkovic, P. M. Jardim, R. R. de Avillez, and F. Rizzo, *Sol. Stat. Sci.* **7**, 1377 (2005).
- ² T. A. Mary, J. S. O. Evans, T. Vogt, and A. W. Sleight, *Science* **272**, 90 (1996).
- ³ J. S. O. Evans, T. A. Mary, T. Vogt, M. A. Subramanian, and A. W. Sleight, *Chem. Mater.* **8**, 2809 (1996).
- ⁴ C. Lind, A. P. Wilkinson, Z. B. Hu, S. Short, and J. D. Jorgensen, *Chem. Mater.* **10**, 2335 (1998).
- ⁵ C. Lind, *Materials* **5**, 1125 (2012).
- ⁶ V. Gava, A. L. Martinotto, and C. A. Perottoni, *Phys. Rev. Lett.* **109**, 195503 (2012).
- ⁷ F. Bridge, T. Keiber, P. Juhas, S. J. L. Billinge, L. Sutton, J. Wilde, and Glen R. Kowach, *Phys. Rev. Lett.* **112**, 045505 (2014).
- ⁸ P. M. Forster and A. W. Sleight, *Int. J. Inorg. Mater.* **1**, 123 (1999).
- ⁹ P. M. Forster, A. Yokochi, and A. W. Sleight, *J. Sol. Stat. Chem.* **140**, 157 (1998).
- ¹⁰ Bojan A. Marinkovic, Monica Ari, Roberto R. de Avillez, Fernando Rizzo, Fabio F. Ferreira, Kimberly J. Miller, Michel B. Johnson, and Mary Anne White, *Chem. Mater.* **21**, 2886 (2009).
- ¹¹ Lei Wang, Fei Wang, Peng-Fei Yuan, Qiang Sun, Er-Jun Liang, Yu Jia, and Zheng-Xiao Guo, *Mater. Res. Bull.* **48**, 2724 (2013).
- ¹² S. Sumithra and A. M. Umarji, *Sol. Stat. Sci.* **8**, 1453 (2006).
- ¹³ N. Duan, U. Kameswari, and A. W. Sleight, *J. Am. Chem. Soc.* **121**, 10432 (1999).
- ¹⁴ M. M. Wu, Y. Z. Cheng, J. Peng, X. L. Xiao, D. F. Chen, R. Kiyonagi, J. S. Fieramosca, S. Short, J. Jorgensen, and Z. B. Hu, *Mater. Res. Bull.* **42**, 2090 (2007).
- ¹⁵ M. M. Wu, J. Peng, Y. Z. Cheng, X. L. Xiao, Y. M. Hao, and Z. B. Hu, *Mater. Sci. Eng. B* **137**, 144 (2007).
- ¹⁶ M. M. Wu, J. Peng, Y. Z. Cheng, H. Wang, Z. X. Yu, D. F. Chen, and Z. B. Hu, *Sol. Stat. Sci.* **8**, 665 (2006).
- ¹⁷ X. L. Xiao, J. Peng, M. M. Wu, Y. Z. Cheng, D. F. Chen, and Z. B. Hu, *J. Alloy. Compd.* **465**, 556 (2008).
- ¹⁸ J. Peng, M. M. Wu, H. Wang, Y. M. Hao, Z. B. Hu, Z. X. Yu, D. F. Chen, R. Kiyonagi, J. S. Fieramosca, S. Short, and J. Jorgensen, *J. Alloy. Compd.* **453**, 49 (2008).
- ¹⁹ S. Sumithra, A. K. Tyagi, and A. M. Umarji, *Mater. Sci. Eng. B* **116**, 14 (2005).
- ²⁰ S. Sumithra and A. M. Umarji, *Mater. Res. Bull.* **40**, 167 (2005).
- ²¹ Erjun Liang, Haolei Huo, Junping Wang, and Mingju Chao, *J. Phys. Chem. C* **112**, 6577 (2008).
- ²² G. Kresse and J. Furthmüller, *Phys. Rev. B* **54**, 11169 (1996).
- ²³ G. Kresse and J. Hafner, *Phys. Rev. B* **47**, 558(R) (1993); **49**, 14251 (1994).
- ²⁴ P. Hohenberg and W. Kohn, *Phys. Rev.* **136**, B864 (1964).
- ²⁵ W. Kohn and L. J. Sham, *Phys. Rev.* **140**, A1133 (1965).
- ²⁶ J. P. Perdew, K. Burke, and M. Ernzerhof, *Phys. Rev. Lett.* **77**, 3865 (1996).
- ²⁷ J. Klimeš, D. R. Bowler, and A. Michaelides, *Phys. Rev. B* **83**, 195131 (2011).
- ²⁸ H. J. Monkhorst and J. D. Pack, *Phys. Rev. B* **13**, 5188 (1976).
- ²⁹ M. Methfessel and A. T. Paxton, *Phys. Rev. B* **40**, 3616 (1989).
- ³⁰ Atsushi Togo, Fumiyasu Oba, and Isao Tanaka, *Phys. Rev. B* **78**, 134106 (2008).
- ³¹ Ann E. Mattsson, Rickard Armiento, Peter A. Schultz, and Thomas R. Mattsson, *Phys. Rev. B* **73**, 195123 (2006).
- ³² Guillaume Poulet, Philippe Sautet, and Emilio Artacho, *Phys. Rev. B* **68**, 075118 (2003).
- ³³ I-Chun Lin, Ari P. Seitsonen, Ivano Tavernelli, and Ursula Rothlisberger, *J. Chem. Theo. Comp.* **8**, 3902 (2012).